Agricultural Water Management 146 (2014) 346–360

Contents lists available at ScienceDirect

Agricultural Water Management

journal homepage: www.elsevier.com/locate/agwat

Sustainability and environmental assessment of fertigation in an intensive olive grove under Mediterranean conditions

M.R. Cameira [a,*], A. Pereira [a], L. Ahuja [b], L. Ma [b]

[a] Department of Biosystems Engineering, Superior Institute of Agronomy, University of Lisbon, Tapada da Ajuda, 1349-017 Lisbon, Portugal
[b] USDA-ARS-NPA, Agricultural Systems Research Unit, Fort Collins, CO, USA

ARTICLE INFO

Article history:
Received 28 December 2013
Accepted 4 September 2014

Keywords:
Irrigation
Olive grove
System modeling
RZWQM2
Water balance
N leaching

ABSTRACT

Water and nitrogen surpluses are major concern for the new intensive olive groves in South of Portugal. In this study, field measurements were integrated with a system model, Root Zone Water Quality Model (RZWQM2) to assess the sustainability and environmental impact of fertigation in an intensive olive grove (*Olea europaea* L. var. *Arbequina*). The model provided acceptable predictions of evapotranspiration, soil moisture and nitrate contents. Based on model simulations, under current fertigation practices, 57% of the irrigation applied was lost *via* drainage, while 71% and 5% of fertilizer N inputs were lost through leaching and denitrification, respectively. The non-fertilizer N input from soil organic matter (OM) satisfied 64% of the crop N needs. The tested model was used to predict the impacts of a full irrigation (FIFC) and two regulated deficit irrigation schemes (RDI75, RDI50) on drainage and N leaching. In FIFC the atmospheric demand was met while the application frequency maintained the water storage below the soil field capacity. In RDI75 and RDI50 the irrigation application amount between stone hardening and onset of ripening was 75 and 50% of FIFC respectively.

Compared with the current practice, the FIFC decreased drainage and N leaching by 47% and 90% respectively, while maintaining the actual evapotranspiration (ETa). The RDI75 seems to be the most adequate for the studied agro-system since, in relation to the FIFC, it saved 13% of irrigation water with only 5% decrease in ETa. Furthermore, the 15% reduction in leaching, together with the 19% increase in soil OM mineralization optimized the trees N uptake. The study of three different N application rates for each irrigation scenario indicated that, to minimize residual storage, N should be applied according to plant needs, by using a real-time indicator based upon foliar analysis or the chlorophyll meter measurements.

1. Introduction

Olive orchards are a key component of agricultural systems of the Mediterranean basin, occupying around 9.5 Mha in 2010, with more than 5 Mha in the European Union (FAOSTAT, 2012). In southern Portugal olive trees have been cultivated in traditional non-intensive or low tree-density orchards (around 200 trees ha^{-1}) with no irrigation. Recently, to take advantage of the European Commission decision 2000/406/CE that expands the Portuguese planting quota together with the new *Alqueva* Irrigation Project in the Alentejo region, drip irrigation has been established to intensive orchards characterized by a high tree-density (300–400 trees ha^{-1}) and super intensive orchards characterized by a very high tree-density (400–1700 trees ha^{-1}). The *Alqueva* Irrigation Project is centered on the *Alqueva* dam, the largest strategic water reserve in Europe, with a catchment area of approximately 10 000 km^2 and irrigating 120 000 ha of land. The Regional Department of Agriculture has estimated a total area of 350 thousand hectares of olive groves for the country, of which close to 160 thousand hectares are irrigated, including 45 thousand hectares occupied by intensive olive groves (RGA2009, 2011). The super intensive olive groves occupy an area of 4000 ha. In Alentejo these groves are installed mainly in Luvisols which are very common soils in Mediterranean climates, representing 20% of the area (approximately 500 thousand hectares) (Azevedo and Cary, 1989).

The replacement of traditional rain fed orchards by highly productive irrigated orchards has resulted in an increase in the use of water and nitrogen (N) fertilizers, possibly bringing environmental problems associated with the water bodies and jeopardizing the sustainability of these new agro ecosystems. This matter has received increasing attention as part of the policy debate and the media. Thereby it is necessary to evaluate the overall environmental impact of these new production systems and if necessary to define alternatives for their management specific to the semi-arid

* Corresponding author. Tel.: +351 21 365 34 78.
E-mail address: roscameira@isa.ulisboa.pt (M.R. Cameira).

http://dx.doi.org/10.1016/j.agwat.2014.09.007
0378-3774/

Mediterranean region. Alternative management practices for the sustainable olive groves must be based on the premises that: the water is scarce in the Mediterranean regions; excessive amounts or poorly distributed water during the crop cycle results in drainage losses and N leaching affecting water quality of the underlying aquifer; and in fertile soils the annual application of N fertilizer has frequently shown to be unnecessary to maintain high productivity and oil quality.

The intensive and super intensive orchards are predominantly irrigated by drip systems which are a key factor in their management. Drip irrigation reduces excessive water and fertilizer applications and associated losses. However, its efficiency could vary with soil types and amounts of water applied while meeting crop water demand or allowing some water stress. In general, irrigation increases the vegetative growth and production of olives, and improves the characteristics of the fruit and the oil. However, no significant differences were found under different irrigation regimes, if a controlled water stress was applied – called the regulated deficit irrigation (RDI) (Tovar et al., 2002; Tognetti et al., 2006; Iniesta et al., 2009; Ramos and Santos, 2010; and Gispert et al., 2013). Water stress early in the season (March to July) may reduce the yield due to effects on flowering and fruit set (Orgaz and Fereres, 2004). The last phase of development (fruit and oil accumulation) is also very sensitive to water deficit (Lavee and Wodner, 1991). However, the middle phase of fruit development, when pit hardening occurs (mid-July to mid-September), is most resistant to water deficit (Iniesta et al., 2009) and is when water supplies can either be reduced or halted (Goldhamer, 1999). Strategies for deficit irrigation in arid/semi-arid areas for the conservation of water resources are then applicable and recommended (Massoud et al., 2003; Ramos and Santos, 2010).

Fernández-Escobar et al. (2009) among others report the accumulation of high amounts of N-NO_3 in the soil of fertilized olive grove plots, representing a high risk of N leaching. As an excess of N can negatively affect olive oil and fruit quality the authors suggest that in fertile soils, the annual application of N fertilizer may be unnecessary to maintain high productivity due to N mineralization from soil organic matter. This will depend upon the soil organic matter (OM) and state variables as soil temperature, soil moisture and aeration (Shaffer et al., 2000). Thus, N balance analysis for different fertigation management practices is critical for the reduction of environmental impacts without significant production losses. The experimental quantification of the OM mineralization and the loss terms of volatilization/denitrification and leaching, for various alternative practices is costly and disruptive of the soil. In this context, mathematical models for the simulation of water and nutrient budgets in the vadose zone, properly calibrated and validated, are an indispensable tool (Ma et al., 2007). Several models have been tested for the prediction of leaching, some of which are used in the management and decision-making with regard to the evaluation of the effectiveness of best management practices (BMPs). They can present one dimensional structure, like DAISY (Hansen et al., 1990), STICS (Brisson et al., 1998), LEACHN (Hutson and Wagenet, 1995), COUP (Jansson and Karlberg, 2004) and NLEAP (Follet et al., 1994) or bi/tridimensional structure like Hydrus (Šimůnek et al., 1999) and FUSSIM2 (Heinen, 2001). Several papers on this subject have been presented (*e.g.* Gärdenäs et al., 2005; Hansen et al., 2006), but none with respect to intensive irrigated olive groves. Several of the models are specialized in crop development and yield prediction, water requirements, soil water fluxes or nutrient budget. However, few embody these aspects holistically producing estimates as a function of the interaction of various types of soil, climate and agricultural practices, as does the Root Zone Water Quality Model 2 (RZWQM2, Ahuja et al., 2000a). RZWQM2 was developed by the USDA and was already validated and used in Portugal for the assessment of the nitrate pollution potential in cereals and vegetables (Cameira et al., 2005, 2007, 2014). It is now applied for the first time to an intensive irrigated olive grove.

The objective of the present work was to develop a model-based management tool for the fertigation of intensive olive orchards in Alentejo region. In particular it was intended to: (1) adapt RZWQM2 for the representation of the olive groves typical of the Mediterranean agro-ecosystem; (2) evaluate its ability to simulate the water and N dynamics in the fertigated olive orchards; (3) assess the environmental impact of the current fertigation practices and to propose alternative management practices.

The applied methodology integrates system modeling and field experiments regarding water and N dynamics in the plant soil atmosphere continuum.

2. Materials and methods

2.1. Experimental site

The experiments were carried out in a 10 ha plot which is a part of a 270 ha commercial olive orchard (*Olea europaea* L. var. *Arbequina*) belonging to an olive oil production company and located in Alentejo, south Portugal (38°1.34′ N, 8°10.84′ W, elevation 97 m). The climate in the region is Mediterranean with an average annual rainfall (2001–2011) of 623.4 mm, of which 80% occurs from October to April (Fig. 1). Daily average air temperature varies from 6 to 17 °C in winter and from 12 to 27 °C during summer. Fig. 1 shows precipitation and temperature values measured during the experimental years as well as reference evapotranspiration (ETo) computed with the FAO-PM method (Allen et al., 1998) using meteorological data collected at a meteorological station near the experimental site (38°2.7′ N, 8°15.98′ W). Annual ETo values for 2010 and 2011 were 1170 and 1148 mm respectively.

The soil is a Luvisol (FAO, 2006), a very common soil in the Mediterranean regions. The soil profile has an argic horizon starting at the depth of 60 cm (Table 1) with a stable structure and a high capacity for available water storage (240 mm m^{-1}). This horizon is overlaid by coarser material with loamy sand texture and an average available water storage capacity of 180 mm m^{-1}. The top 30 cm present a moderate OM content of 15 mg g^{-1}. Measured saturated hydraulic conductivity (K_{sat}) shows a moderate to high value of 5.1 cm h^{-1} for the top soil layer, decreasing to a low value of 0.5 cm h^{-1} in the 60–100 cm layer in association with the increase in clay content. The soil has moderate/good drainage based on visual observations.

The olive trees were planted in 2004 with a 7 m × 4.8 m spacing (≈300 trees ha^{-1}, which is considered as an intensive production system). The evergreen trees present limited activity during winter (semi-dormancy) and initiate vegetative growth in early spring. The orchard was irrigated by a drip system using water from the Alqueva Irrigation Project. The experimental plot, with an area of 10 ha, was served by an independent irrigation sector consisting of seven drip lines (UniRam™ by Netafim, Fresno, CA) each with a length of 200 m. A single drip line, was placed on the soil surface in each tree row. Each tree was serviced by six pressure compensating emitters, spaced 0.75 m, and each discharging 1.6 L h^{-1}. Irrigation was applied daily from May to October during the period of higher water demand, according the local practice based upon the farmers' empirical knowledge. N fertilization was also performed according to the standard practice followed by local growers, using a N–P–K fertilizer delivering 8–11% N (50% ammonium and 50% nitrate) injected into the system and applied with the irrigation water. Total irrigation and N fertilization amounts and distribution through the season are presented in Table 2.

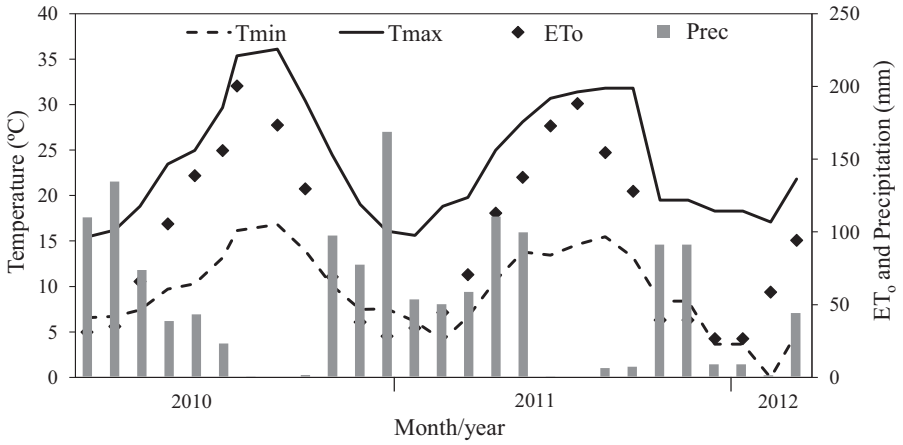

Fig. 1. Monthly precipitation (Prec) and reference evapotranspiration (ET_o), daily average maximum (Tmax) and minimum temperatures (Tmin) for the experimental site during the period of study (01/2010–03/2012).

Table 1
Physical properties measured from soil samples or *in situ*.

Depth	Particle size (%)			BD (g cm^{-3})	θ_v (cm^3 cm^{-3})		K_{sat} (cm h^{-1})
(cm)	Sand	Silt	Clay		10 kPa	1500 kPa	
0–30	84.5	7.9	7.6	1.46	0.24	0.06	5.1
30–60	85.4	6.9	7.7	1.46	0.25	0.06	3.6
60–100	70.3	6.0	23.7	1.42	0.34	0.10	0.5

BD is the bulk density; θ_v is the volumetric water content; K_{sat} is the saturated hydraulic conductivity; θ_v at 10 and 1500 kPa represent field capacity and wilting point respectively.

2.2. Modeling

2.2.1. Modeling strategies

RZWQM2 simulates agricultural management effects on crop production and environmental quality. Although it is a one-dimensional model, RZWQM2 was chosen to simulate the olive grove drip fertigated agro system because: (i) RZWQM2 contains important process interactions within the agricultural system that the existing 2D or 3D soil water models do not present; and (ii) the modeling was not intended to simulate the highly accurate soil moisture 3D redistribution pattern after irrigation, but rather an overall soil water and N balance for environmental assessment of the management practices. Due to the 1D characteristic of RZWQM2 two independent simulations were performed, one in the area receiving irrigation water and the other in the non-irrigated soil, where the water inputs were from precipitation only. This way it was possible to identify drainage and leaching associated with the group of emitters serving one tree and to relate these losses with the management inputs. When a global result was wanted, the results from both simulations were weighted according to the relative proportion of each area.

2.2.2. RZWQM2 overview and general model parameterization

RZWQM2 includes several components or modules (Ahuja et al., 2000a; Ma et al., 2012) whose processes and parameterization are briefly described below. The general model inputs associated with each process and type of data sources used for this study are summarized in Table 3.

The soil water module uses the Green–Ampt (Green and Ampt, 1911) equation for infiltration during irrigation or rainfall events and the Richards' equation (Celia et al., 1990) for water redistribution in the soil between events. Plant water uptake is simulated with the Nimah–Hanks equation (Nimah and Hanks, 1973) and coupled to the Richards' equation as a sink term. The modified Brooks–Corey equation is used to describe the soil water retention curve and the hydraulic conductivity curve (Ahuja et al., 2000b).

The potential evapotranspiration (ETp) calculation in RZWQM2 (Farahani and DeCoursey, 2000) is based on the Shuttleworth and Wallace (S-W) dual surface version of the Penman–Monteith equation (Shuttleworth and Wallace, 1985). This approach is used only to compute the ETp rate, while the actual evapotranspiration rate (ETa) is obtained through the soil water transport model described above.

Table 2
Irrigation and N fertilization distribution during the fertigation season.

Year	May	June	July	August	September	October	Total	
	Irrigation, % total						mm	m^3 tree^{-1}
2010	6	14	20	27	26	7	154	5.1
2011	–	19	29	29	21	2	142	4.8
Year	May	June	July	August	September	October	Total	
	N Fertilization, % total						kg ha^{-1}	kg tree^{-1}
2010	19	39	23	19	–	–	65	0.218
2011	18	31	28	23	–	–	68	0.228

Table 3
General model inputs and data source type.

Module Parameter	Data source
Soil water	
Soil texture, bulk density, 10 kPa and 1500 kPa suction water content and saturated hydraulic conductivity	Measured
Brooks and Corey soil water retention and hydraulic conductivity parameters	Estimated
Crop and evapotranspiration	
Tree height and maximum rooting depth	Measured
Leaf area index, minimum stomata resistance, plant canopy albedo	Literature
Soil organic matter and N	
Potential seasonal N uptake	Literature
Soil organic matter	Measured
Organic pools partitioning and interpool transfer coefficients	Estimated
Nitrification rate constant	Literature
Management practices	
Plating density, row spacing, length of the active and semi-dormant periods	Measured
Irrigation dates and amounts	Measured
Fertilization dates and amounts	Measured

Estimated means calculated using measured properties and an adequate estimation methods as explained in the text.

The organic matter and nitrogen (OMNI) module was developed to simulate soil carbon (C) and nitrogen (N) transformations (Shaffer et al., 2000). It simulates the major pathways of the soil C/N dynamics including mineralization–immobilization, ammonia volatilization and nitrification. Organic matter (OM) is distributed over five computational pools and decomposed by three microbial mass populations. The OM pools consist of slow and fast pools for crop residues and fast, medium and slow pools for soil humus. First-order decomposition rates for each organic C pool are assumed, with rate coefficients as functions of soil temperature, soil oxygen concentration, soil C substrate amount, soil pH, and soil moisture. Plants take up both ammonium and nitrate in proportion to their concentrations present in each soil layer.

At present the RZWQM2 does not include a production model for shrubs or trees. A simplified empirical model, *Quicktree*, was developed by the RZWQM2 team to uptake water and N from the soil. Based upon the input data presented in Table 3, the *Quicktree* module calculates daily values of N uptake by assuming a linear increase of N uptake in the first half of the growing season and a linear decrease in the second half of the growing season. Users can specify when the maximum daily N uptake is taking place. Maximum LAI is also assumed to be in coordination with maximum daily N uptake. The *Quicktree* module was first used by Nolan et al. (2010) to study N leaching in an almond orchard in California, USA, but it has not been applied for olive trees and under the Mediterranean environment. Changes were made to this module in order to adapt it to this situation.

2.2.3. RZWQM2 calibration and validation

The model was calibrated by trial-and-error for a period including one active and one semi-dormant period of the olive grove, involving experimental data from March 14th 2010 to March 13th 2011. The methodology to obtain the calibrated hydraulic properties parameters necessary to characterize the water dynamics within the vadose zone and to estimate the drainage behavior of the soil consisted of:

(i) experimental measurement of basic soil physical properties such as soil texture, bulk density (BD), volumetric moisture (θ_v) at 10 kPa and saturated hydraulic conductivity (K_{sat});
(ii) estimation of the $\theta(h)$ and $K(h)$ curves, based upon the above referred properties. The extended similar media approach was used to derive the Brooks and Corey parameters for $\theta(h)$ (Warrick et al., 1977; Ahuja et al., 1985). The textural class mean of parameters (Rawls et al., 1982) were used to represent the reference curve from which the new scaled curve parameters were obtained. Given the measured K_{sat} and the estimated $\theta(h)$ functions, the unsaturated conductivity/suction relationship, $K(h)$, was then estimated by the approximate capillary-bundle approach of Campbell (1974);
(iii) calibration of the measured/estimated $\theta(h)$ and $K(h)$ parameters by inverse modeling against data from an infiltration-redistribution field experiment in bare soil without the interference of root water uptake. First the observed infiltration time and soil moisture contents immediately following water penetration were used to calibrate the driving parameters for infiltration (K_{sat} and θ_s); and then the redistribution soil moisture profiles observed for 2 weeks were used to calibrate the parameters describing the hydraulic functions for non-saturated conditions.

Then the trees were included in the simulated system, and the water balance components for the olive grove were calibrated involving some of the parameters that influence potential evapotranspiration. The control variables for the calibration of the water related processes were (i) the temporal series of volumetric soil moisture (θ_v) measured at different depths and (ii) actual evapotranspiration (ETa) measured during the olive grove active periods.

Finally the calibration of the soil organic matter and N component involved:

(i) Organic pools partitioning. The initial soil organic C pools was set based on measured soil organic matter content at each soil depth using the wizard provided in RZWQM2 and after running the model for a period of 10 years under the current management practices in order to equilibrate the humus and microorganisms pools (Ma et al., 2011).
(ii) the interpool transfer coefficients, for the accurate simulation of the mineralization rate;
(iii) the nitrification rate constant, in order to accurately simulate the transformations of the ammonium present in the fertilizer.

The control variables for (i) and (ii) were the expected annual N mineralization and N supply to the soil, estimated from Schepers and Mosier (1991). For (iii) the control variables were the temporal series of soil nitrate measured at different soil depths.

Model calibration was conducted in the order of soil water dynamics, evapotranspiration, soil nitrogen, and iterated several times in the same order to minimize error propagation between modules. Model validation was performed using independent soil moisture, soil N and ETc data collected from 14th March 2011 to 13th March 2012 under the current management practices. During this phase the previously calibrated parameters were not changed.

The goodness of the predictions for the water and N components was evaluated by the following statistics: root mean squared error (RMSE) compared with the mean standard deviation of the measurements (MSD), coefficient of determination (r^2), Nash–Sutcliffe modeling efficiency (EF) (Nash and Sutcliffe, 1970) and D index (Willmott, 1981). The r^2 value ranges from 0 to 1, where the value of 1 indicates a perfect correlation between experimental and simulation results and the value of 0 means no correlation between the two results. The use of this approach alone can be misleading, as it does not account for a systematic bias. Therefore it should

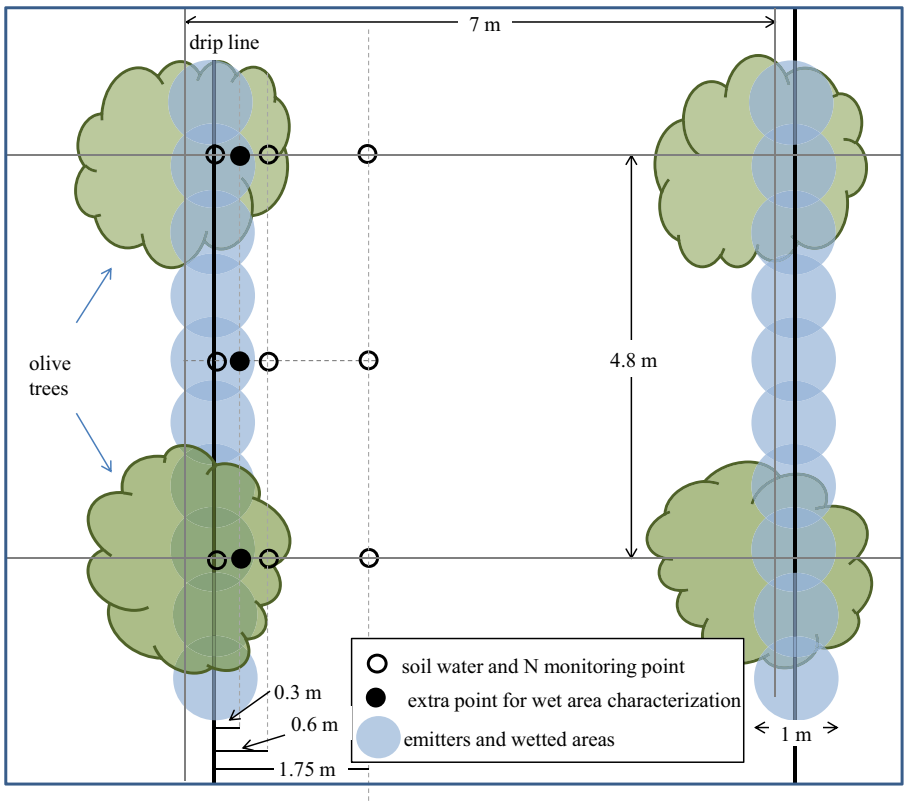

Fig. 2. Experimental layout, replicated randomly within the studied plot in each sampling day.

be used only for trend analysis. EF is a measure of the deviation between model predictions and measurements in relationship to the scattering of the observed data. EF = 1 indicates a perfect match between simulation and observed results. The *D* index is similar to EF but more sensitive to systematic model bias. As their values move away from 1, model calibration becomes worse. For soil water and N-related calibrated predictions the expected minimum values for EF, *D* and r^2 are 0.7, 0.7 and 0.8 respectively (Ma et al., 2011). With respect to validation usually only the RMSE is used and compared to MSD, although the complete set of statistics is being presented for both modeling phases.

2.3. Experimental setup and measurements

The experimental set up was design in order to characterize the system to be modeled and to obtain data to calibrate and validate the model, as described in the above section. Experiments began in March 2010 and continued until March 2012, including two fertigation seasons with the objective of collecting data for the calibration (2010/2011) and validation (2011/2012) of the RZWQM2. Fig. 2 presents a monitoring area, showing the relative position of the olive trees, the emitters and the soil sampling locations.

2.3.1. Soil physical properties

Before the start of irrigation season a soil profile was exposed for soil characterization. Soil samples were collected at the depths of 0–30, 30–60 and 60–90 cm for analysis of particle size distribution (soil texture), bulk density (BD), soil moisture at 10 kPa (field capacity, FC) and 1500 kPa (wilting point, WP). The K_{sat} was measured *in situ*, at the same depths, by the double ring infiltrometer method (Bouwer, 1986) as the profile was being exposed.

The infiltration/redistribution experiment was carried in a 3 m^2 area, where an EnviroSCAN probe (Sentek Pty. Ltd, Stepney, South Australia) was installed and connected to a Sentek Enviroscan RT6 data logger. A volume of 360 L of water was applied uniformly in order to saturate the soil profile beneath this area. After infiltration the soil was covered with a plastic film to prevent fluxes through the soil surface. Data were collected continuously during 2 weeks, until soil moisture showed no significant variations. Details about a similar experiment are presented in Cameira et al., (2000).

2.3.2. Irrigation and crop measurements

The exposed soil profile allowed the observation of the root system extent both laterally and in depth. Tree height and canopy diameter were measured at nine randomly selected trees.

Irrigation application amounts were measured with a tipping-bucket raingaugue (ARG100, Environmental Measurements Ltd, Sunderland, UK) connected to a data logger (CR1000, Campbell Scientific, Inc, Logan, UT, USA). Observation of the soil surface indicated that the wetted areas associated with each emitter intersected, forming a wet band along the tree rows, presenting a width of approximately 1.0 m (Fig. 2). Average depth and width of the wetted areas were estimated from the soil moisture content measured using the gravimetric method at three depths (15, 45 and 75 cm) and at three distances (0, 30 and 60 cm) from the emitter on three dates: before the irrigation season, at the beginning and at the middle of the irrigation season. The gravimetric method results were later multiplied by the soil bulk density in order to obtain volumetric water contents. Irrigation water samples were collected at the source two times during the season for the quantification of the N supplied by the irrigation water.

2.3.3. Time series of soil moisture, soil nitrate and actual evapotranspiration

Field measurements of soil moisture, soil N and ETa started in March 2010, at the beginning of the olive trees active growing period. During the first year data was collected for model calibration. The procedures were repeated in the following year, starting

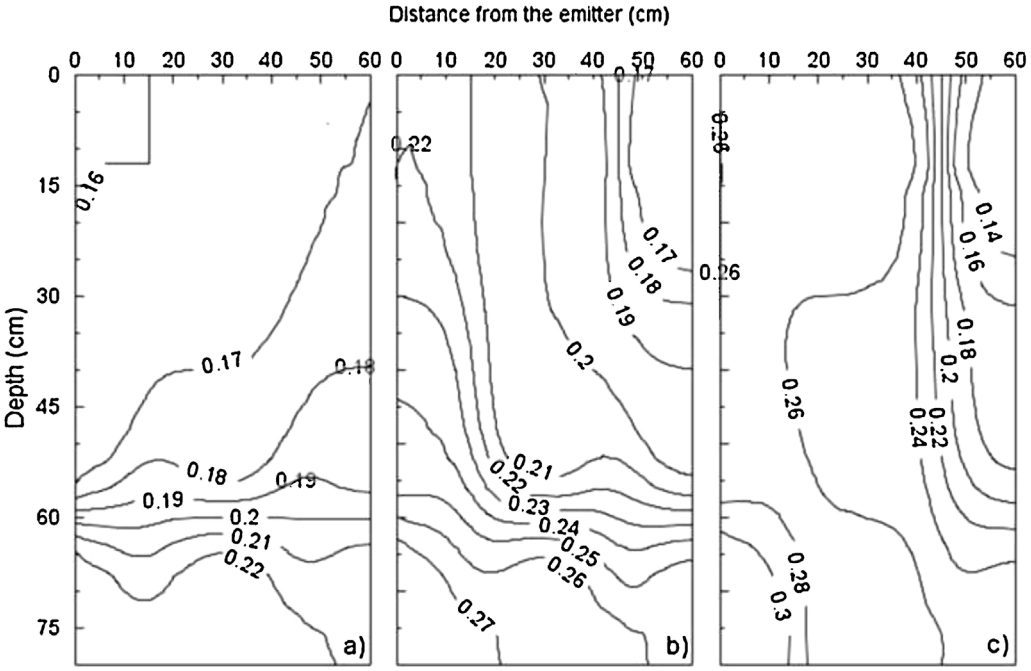

Fig. 3. Representation 2D of soil moisture, where the origin marks the emitter position, for three dates: (a) before the irrigation season, (b) in the beginning and (c) in the middle of the irrigation season (2010).

in the beginning of the new active growing period (March 2011) in order to collect data for the independent model validation.

Soil samples were collected, using a 150 cm long and 5 cm diameter auger, at 0–30 and 30–60 cm soil depths in order to characterize the soil layer with the presence of roots and at 60–90 cm depth in order to monitor water and N movement below the root zone. The samples were collected perpendicularly to the tree rows at three distances from the emitter (0, 60 and 175 cm) in order to gather information from both the irrigated and the non-irrigated areas (Fig. 2). Samples were collected during the two experimental years with a variable frequency depending upon the period (irrigation season or not) and the objective (calibration or validation). For each measurement day the sampling area presented in Fig. 2 was replicated twice randomly in the grove, yielding nine samples per depth and per distance from the emitter. Each soil sample was divided into two subsamples. One subsample was stored in plastic bags and frozen for soil NO_3-N analysis, where soil NO_3-N was extracted with a 2.3 M KCl solution and concentration was calculated using the segmented flux method (Maynard and Kalra, 1993). The other subsample was used for the determination of the soil moisture by the gravimetric method. The results were later multiplied by the soil bulk density in order to obtain volumetric water contents.

Data collection for the determination of actual evapotranspiration started in June 2010. Measurements were performed by Conceição and Ferreira (2013) by applying a method consisting of long term continuous Granier sap flow measurements related to short periods of eddy covariance measurements. The method is described in detail by Ferreira et al. (2004), Silva et al. (2008) and Paço et al. (2012).

3. Results and discussion

3.1. Model parameterization and calibration

3.1.1. Root distribution and wetted zone dimensions

Highest root densities were found in the top 35 cm soil layer mainly close to the trunk. More roots, including those of smallest diameter, were found down to 60 cm depth and as far as the vertical projection of the canopy. Very rare roots were observed down to 90 cm depth. This shallow root distribution pattern is typical for the olive tree drip irrigated since planting (Fernández et al., 1991; Morales-Sillero et al., 2009). In RZWQM2 the bottom of the root zone was then considered to be at the depth of 60 cm, and the drainage/leaching breakthrough depth was set at 90 cm to account for possible activity between 60 and 90 cm depth.

Table 4
Measurements and calculations relative to the crop and the irrigation system.

Crop		Irrigation	
Tree height (m)	2.5 ± 0.36	Emitter discharge ($L\,h^{-1}$)	1.6 ± 0.14
Canopy diameter (m)	2.5 ± 0.20	Wet band width (m)	0.5 ± 0.1
Ground cover (%)	15	Wetted area (%)	15
Rooting depth (m)	0.6	NO_3-N in water ($mg\,L^{-1}$)	5

Fig. 3 presents the soil moisture contour lines obtained by interpolation of the measurements. Before the irrigation season (Fig. 3a) the soil moisture pattern was relatively uniform in depth and laterally. Few days after the beginning of the irrigation season (Fig. 3b) soil moisture reached field capacity vertically down to the depth of 60 cm. Laterally irrigation water reached a distance between 40 and 50 cm from the emitter. In the middle of the irrigation period (Fig. 3c) the wetted distance at surface still did not exceed 50 cm, while in depth all the profile was at field capacity. Thus, the wetted band was approximately 100 cm wide, and the irrigated area associated to a tree was estimated to be ≈5 m^2. This corresponds to approximately 15% of wetted area and 85% of non-irrigated area. Table 4 presents the results obtained from crop and irrigation measurements and used to parameterize the model.

3.1.2. Soil hydraulic properties

Table 5 shows the Brooks and Corey functions and correspondent parameters before and after calibration. Both the original and

Table 5
Parameters of the Brooks and Corey functions that describe the soil hydraulic properties, estimated and calibrated against the infiltration/redistribution experiment.

Depth	0–60 cm		% change	>60 cm		% change
Parameter	Estimated	Calibrated		Estimated	Calibrated	
θ_s ($cm^3\ cm^{-3}$)	0.449	0.390	13	0.460	0.400	13
λ	0.35	0.30	14	0.5	0.8	60
$\theta_{10\ kPa}$ ($cm^3\ cm^{-3}$)	0.196	0.210	7	0.349	0.280	19
$\theta_{1500\ kPa}$ ($cm^3\ cm^{-3}$)	0.067	0.079	18	0.156	0.100	35
K_{sat} ($cm\ h^{-1}$)	5.1	6.1	20	0.5	0.8	60
N_2	3.50	3.20	9	2.75	2.84	3
h_b (cm)	6.47	10.45	61	6.47	24.5	61

θ_s is the saturated soil water content, λ is the slope of the $\log(\theta)$–$\log(h)$ curve, $\theta_{10\ kPa}$ and $\theta_{1500\ kPa}$ represent the field capacity and the wilting point respectively, K_{sat} is the saturated hydraulic conductivity, N_2 is the slope of the $\log(K)$–$\log(h)$ and h_b is the air entry water pressure.

the calibrated curves reflect the existence of a layer with clay accumulation starting at 60 cm, typical for the Luvisol (Table 1), presenting a higher θ_s, lower K_{sat}, and higher pore size distribution index (λ) in comparison with the upper layer. Therefore, it has a higher water retention capacity and a lower permeability in relation to the overlying soil. The calibrated parameters for the layer 0–60 cm show, in relation to the original estimated ones, an increase in the water retention capacity (decrease in λ) and hydraulic conductivity (decrease in N_2) for high suctions. Bubbling pressure increased toward a more heavy textured soil. These parameters reflect the high fine sand content of the soil, with hydraulic properties closer to silt than to coarse sand. As to the argic horizon, the calibrated $K(h)$ was almost unchanged while the $\theta(h)$ changed toward a slightly lower retention soil. Containing less sand, this soil horizon is more prone to structure disturbance during sampling for the soil moisture determination at 10 kPa, thus showing higher percentage changes than the surface horizon. The soil moisture profiles obtained during the calibration process after infiltration and after 1 and 7 days of redistribution are shown in Fig. 4a, showing a good adjustment between predicted and observed data. Fig. 4b shows RZWQM2 predicted *vs* measured θ_v, and the correspondent r^2. As the soil moisture depletion was due to the downward movement of water without the influence of upward fluxes through the soil surface or root uptake, soil moisture variations are very small and uniform over time. As a consequence, in this type of experiment high values of r^2 are usually obtained after the hydraulic parameters' calibration.

3.1.3. Crop parameters and potential evapotranspiration

When the trees were included in the system the ETp prediction was analyzed. Since the model imposed a LAI of zero at the beginning of development, the underestimation of LAI during the initial development stage was causing an overestimation in both the mean canopy boundary layer resistance and the bulk stomatal resistance of the canopy causing large errors in the prediction of transpiration (T). To correct this, the following changes were introduced in the *Quicktree* model before the calibration of the ETp module: (i) parameterization of LAI requiring the initial and the maximum value; (ii) adaptation of the stomatal resistances range considered by the model to the large values presented by species adapted to arid and semi-arid climates; (iii) consideration of the large inter row distance, typical for these Mediterranean groves, with impacts in the ETp partition between transpiration (T) and evaporation (E). The crop and ETp models were then calibrated. Table 6 shows the initial values, measured or estimated from literature and the calibrated parameters. The initial value for the maximum leaf area index (LAI) was selected from the literature (*e.g.* Iniesta et al., 2009), for olive groves under conditions similar to those of the present study. Mariscal et al. (2000) provided values for the albedo of olive trees between 0.09 and 0.12. Based upon Xiloyannis et al. (2000) and Fernández-Escobar et al. (2012), seasonal crop N uptake was assumed to be 140 g N $tree^{-1}$ $year^{-1}$, corresponding to approximately 42 kg N ha^{-1}. The Shuttleworth–Wallace ETp model was very sensitive to the stomatal resistance. The initial default value of 400 s m^{-1} was used while the calibrated value was 700 s m^{-1},

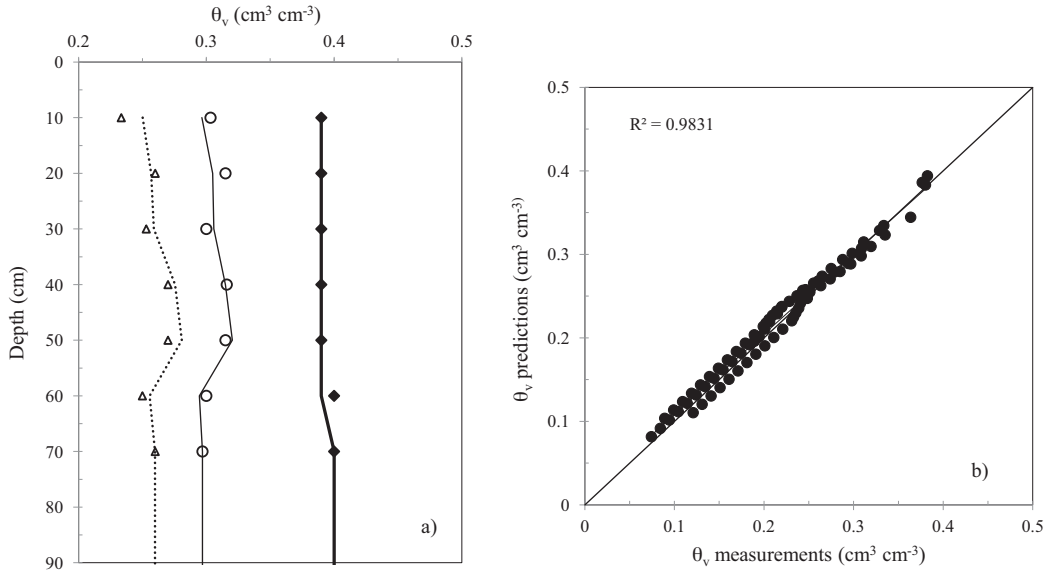

Fig. 4. Hydraulic properties calibration results: (a) soil moisture profiles immediately after, one day and 1 week after infiltration; (b) predicted *vs* observed volumetric soil moisture content (θ_v) for the 2 week redistribution experiment (♦, measured after infiltration; o measured one day after infiltration; △, observed 1 week after infiltration; -----, predicted after infiltration; predicted one day after infiltration, - - - - -, predicted 1 week after infiltration).

Table 6
Crop and ET_P parameterization and calibrated parameters.

Crop parameter	M/E	C	ET_P parameter	M/E	C
Tree height (m)	2.5 ± 0.36	2.5	Albedo of leaves	0.09–0.12	0.15
Rooting depth (m)	0.6	0.7	Albedo of soil	0.25	0.59
LAI	1.0	1.1	Minimum stomatal resistance (s m^{-1})	400	700
Dormant recovery date	74	74	Surface soil resistance (s m^{-1})	200	500
Active period (days)	269	269			
Seasonal N uptake (kg ha^{-1})	42	42			

LAI is the leaf area index, ETp is the potential evapotranspiration, M/E are measured or estimated values, C are calibrated values.

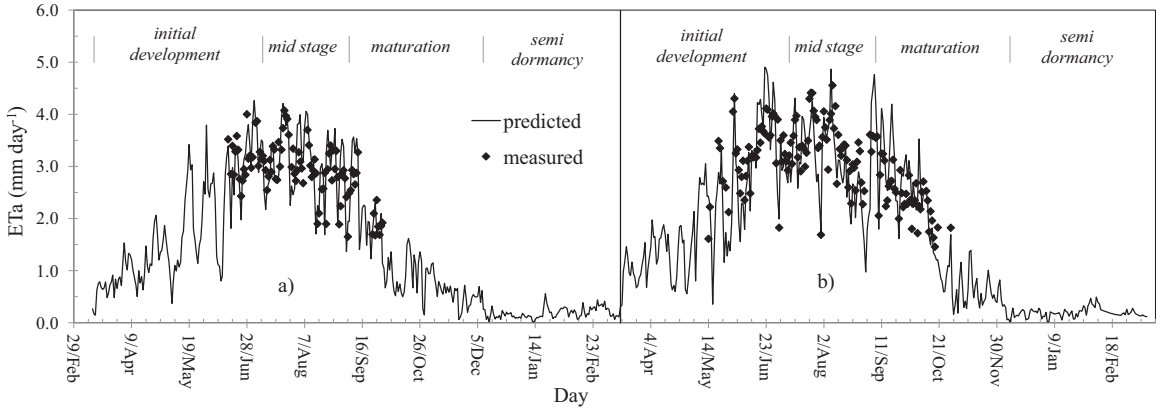

Fig. 5. Predicted and measured actual evapotranspiration (ETa): (a) calibration (2010/2011) and (b) validation (2011/2012).

Table 7
Statistics for the actual evapotranspiration (ETa) prediction for calibration (2010/2011).

RMSE (mm)	MSD (mm)	EF	*D*	r^2
0.45	0.58	0.68	0.88	0.83

RMSE per development phase

Development stage	n_{ob}	RMSE (mm)
Initial development	23	0.40
Mid-season	53	0.50
Maturation	13	0.46

RMSE is the root mean squared error, MSD is the mean standard deviation of the measurements, EF is the modeling efficiency, *D* in the *D* index, r^2 is the coefficient of determination, n_{ob} is the number of observations.

reflecting the species adaptation to semi-arid conditions (Villalobos et al., 2000; Torres-Ruiz et al., 2013). Initial values for soil albedo were obtained from Farahani and DeCoursey (2000), according to soil type, OM content and color. The calibrated values for soil albedo were higher than the initial ones, which is related with the low evaporation since 85% of the soil surface is not affected by irrigation. The same applies to the soil resistance. As there were no measured values for evaporation, during the calibration process soil evaporation in the irrigated zone was maintained between the range indicated by Bonachela et al. (2001) and Testi et al. (2004) for similar conditions of ground cover and wetted area. This yielded 30% ETp for E and 70% ETp for T. Fig. 5a shows the evolution of actual evapotranspiration measured and predicted by the Nimah and Hanks equation using the calibrated ETp as upper boundary condition, for 2010/2011. The model clearly simulated the temporal tendency as well as the peaks associated with specific climatic conditions for some days. Table 7 shows the statistics for the ETc predictions for the calibration period. The RMSE of the simulation was 0.45 mm for the 1-year cycle, which is lower than the mean standard deviation of the measurements. RMSE shows different values for each development stage with higher values for the mid-season. The *D* index and the r^2 present the minimum required values, indicating that both the trend and the magnitude of the results are being predicted with a good accuracy. These results are considered very good for the water balance objective. Similar statistics were presented by Er-Raki et al. (2010), with RMSE values of 0.24 mm and 0.71 mm for E and T estimation by the FAO56 methodology (Allen et al., 1998).

3.1.4. Soil moisture

Fig. 6 shows predicted and measured soil moisture after the calibration of ETp for the irrigated areas between spring 2010 and spring 2011, including both the active and the semi-dormancy periods. Each value represents the average of nine samples associated to the standard deviation of the measurements. During the initial development stage there was a significant increase in soil moisture in all soil layers due to rainfall up to early May. During this phase the root uptake was still low, and θ_v exceeded FC for some days, resulting in the occurrence of drainage to the lower layers. During mid-season, with the increase in ETa soil moisture content ceased to increase in the root zone but remained close to the FC due to the high frequency irrigations. We can assume, therefore, that water availability was not a limiting factor. Whenever θ_v exceeds FC the hydraulic conductivity increases considerably, originating drainage to the subjacent layers, which is the most common situation occurring after rainfall from October 2010 to March 2011. On the other hand, for effective pressure values below 10 kPa (FC) the hydraulic conductivity was low, and even with high gradients there will be no hydraulic fluxes to the deepest layers of the profile. In the 60–90 cm soil layer, soil moisture content increased slowly and continuously over the study period, indicating that irrigation water reached depths beyond the root zone. The same happens for some precipitation events outside the irrigation season. Fig. 7 shows calibration results for the non-wetted areas of the irrigated treatments. Soil water depletion occurred mainly from July to October due to evaporation and the lack of precipitation. After this, soil moisture started to increase due to the winter rainfall. Table 8 presents the statistics for soil moisture prediction. For the irrigated areas the RMSE values are always lower than

Table 8
Statistics for the soil moisture and N predictions for calibration (2010/2011).

Depth (cm)	Irrigated area					Non-irrigated area				
	Soil moisture predictions									
	RMSE ($cm^3\ cm^{-3}$)	MSD ($cm^3\ cm^{-3}$)	EF	D	r^2	RMSE ($cm^3\ cm^{-3}$)	MSD ($cm^3\ cm^{-3}$)	EF	D	r^2
0–30	0.011	0.038	0.84	0.96	0.93	0.019	0.014	0.80	0.95	
30–60	0.013	0.022	0.86	0.96		0.018	0.012	0.74	0.92	0.87
60–90	0.012	0.023	0.88	0.97		0.019	0.018	0.58	0.91	
Depth (cm)	Soil N predictions									
	RMSE ($kg\ ha^{-1}$)	MSD ($kg\ ha^{-1}$)	EF	D	r^2	RMSE ($kg\ ha^{-1}$)	MSD ($kg\ ha^{-1}$)	EF	D	r^2
0–60	5.1	8.0	0.93	0.96	0.96	2.4	2.3	−1.35	0.65	0.52
60–90	3.3	7.5	0.94	0.97		2.9	2.2	−0.80	0.75	

RMSE is the root mean squared error, MSD is the mean standard deviation of the measurements, EF is the modeling efficiency, D in the D index, r^2 is the coefficient of determination calculated for the entire profile (0–90 cm).

the MSD, as required. For the non-irrigated areas RMSE are very close, but higher than the MSD, due to the lower variability of soil moisture measurements in the dryer soil. D index always presents values higher than the minimum recommended (70%). EF presents higher values than the minimum recommended (70%) except for the lower depths in the non-irrigated area. The r^2 presents, for the two situations, higher values than the minimum recommended (0.8). It is concluded that the observed data is being conveniently explained by modeling both in terms of trends and magnitude, and so the model is considered calibrated for the components soil water storage and crop ETa. It can be assumed that the bottom boundary flux (drainage), for which there are no measurements, is being predicted with a similar level of confidence as the measured ETa and water storage.

3.1.5. Soil C/N dynamics

Acording to Scheppers and Mosier (1991) the annual N mineralization should be around 20 $kg\ ha^{-1}\ year^{-1}$ per each 1% of soil endogenous OM, for the top 30 cm. Since the studied soil presented 1.5% OM, calibration aimed at an estimated mineralization

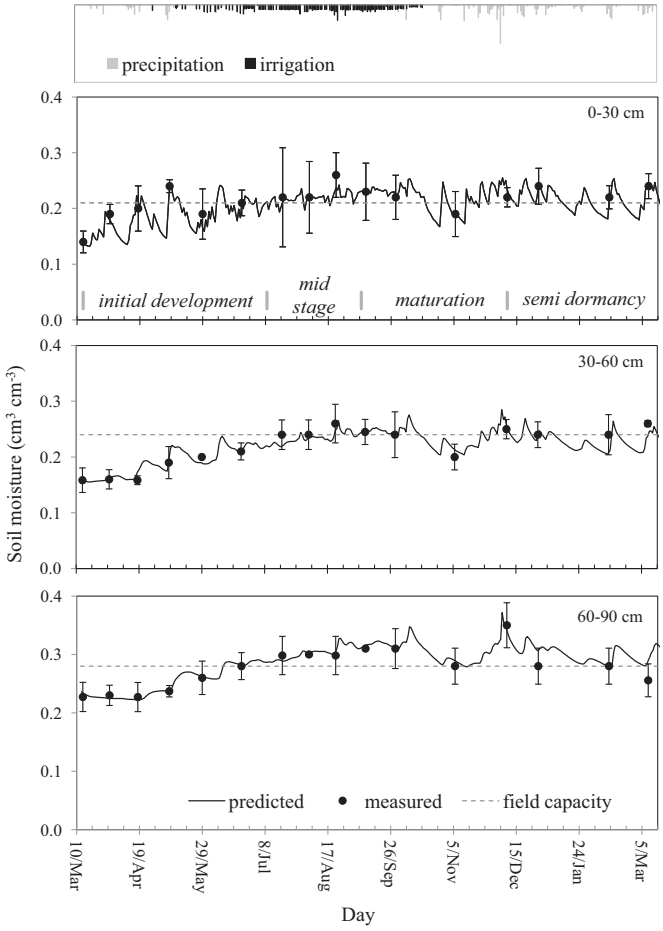

Fig. 6. Predicted and measured soil moisture in the root zone and in the subjacent layer of the irrigated area for calibration (March 2010–March 2011).

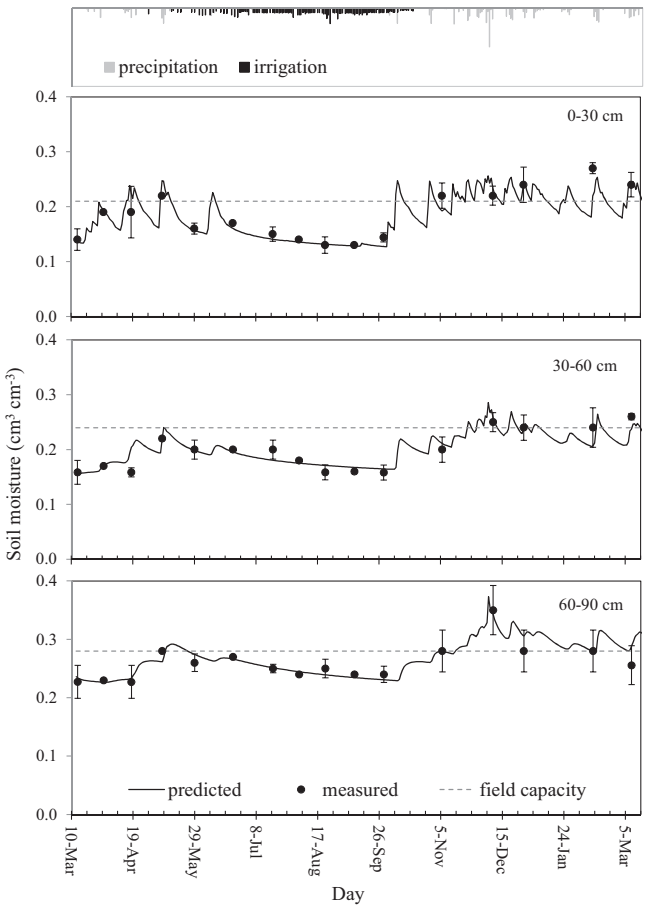

Fig. 7. Predicted and measured soil moisture in the non-irrigated zone for calibration (March 2010–March 2011).

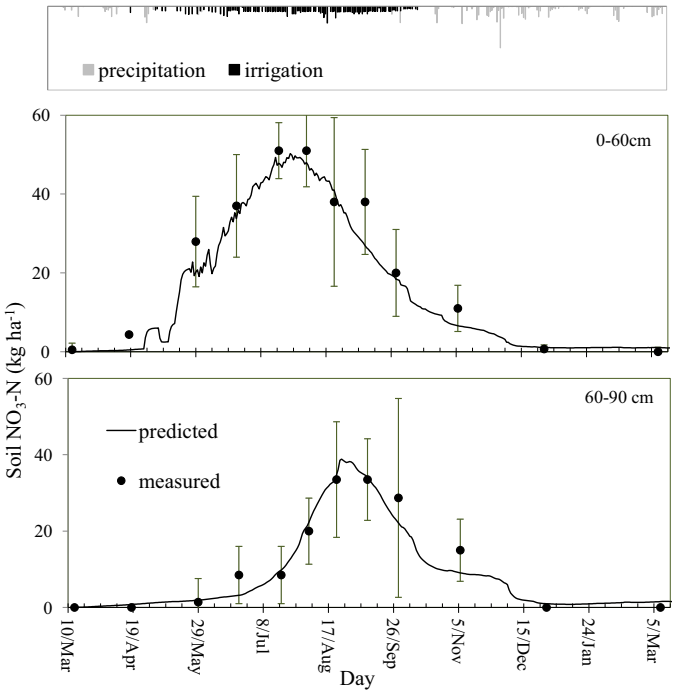

Fig. 8. Predicted and measured soil moisture in the root zone and in the subjacent layer of the irrigated area for validation (March 2011–March 2012).

rate of 30 kg N ha^{-1} $year^{-1}$. To achieve this, the OM was partitioned between the three humus pools as follows: 4% in the fast pool, 16% in the intermediate pool and 80% in the slow humus pool. Then the interpool coefficients were adjusted, resulting in a value of 0.1 between the slow residue and the intermediate soil humus, 0.1 between the fast residue and the fast soil humus, 0.4 between the fast and the intermediate soil humus and 0.4 between the intermediate and the slow soil humus. Then, to adjust the fertilizer NH_4^+ transformation to NO_3^-, the nitrification rate constant was set to 1×10^{-5}. Fig. 8 presents the observed and the predicted NO_3-N storage in the root zone and in the subjacent layer for the irrigated areas, after calibration. Each value represents the average of nine samples associated to the standard deviation of the measurements. NO_3-N started to accumulate in the root zone (0–60 cm) at the beginning of fertigation in late April, while the subsurface layer (60–90 cm) showed significantly lower storage. However at the time the soil moisture reached field capacity (Fig. 6) soil NO_3-N started to decrease in the root zone and to increase in the subsurface layer, indicating the occurrence of N leaching. There is a 30 day lag time for peak occurence in the two soil layers. At the end of the irrigation season (mid-October), when the crop uptake for water and N was low, the soil profile stored 20 kg ha^{-1} of NO_3-N. With the occurrence of the autumn precipitation this NO_3-N disappeared from the soil profile with leaching as the most probable cause. This moderate/high nitrate mobility can explain the almost null concentrations of this compound before the start and at the end of the fertigation period. In the non-irrigated area (Fig. 9) there was an increase of NO_3-N storage in the soil probably due to mineralization of OM. However, this storage was leached out of the root zone with the autumn precipitations. Figs. 8 and 9 show that the model predicted the evolution of NO_3-N storage, including the occurrence of peaks, in both soil layers of the irrigated and non-irrigated areas. Table 8 presents the correspondent statistics. The RMSE values are always lower than the MSD for the irrigated zone. For the non-irrigated zone RMSE is very close but higher than the MSD. *D* index always presents values higher than the minimum recommended (70%). EF presents higher values than the minimum

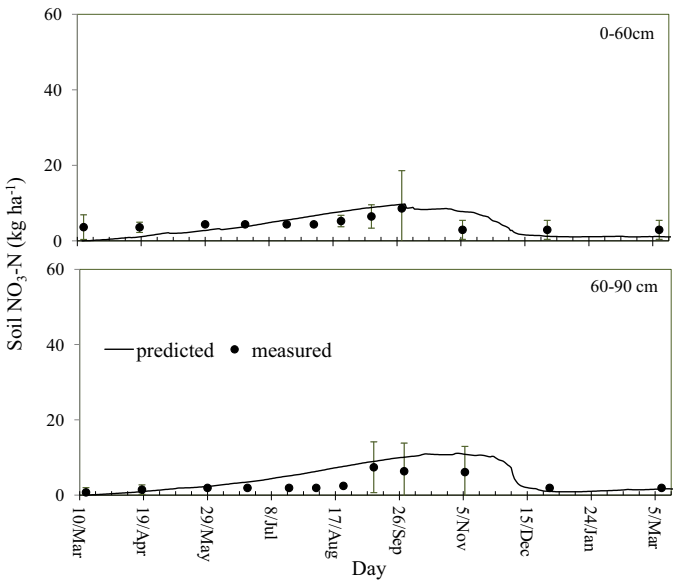

Fig. 9. Predicted and measured soil moisture in the non-irrigated zone for validation (March 2011–March 2012).

recommended (70%) for the irrigated areas. For the non-irrigated areas the negative EF values suggest that the prediction error is higher than the variability of measurements, which, according to Fang et al. (2012) and Youssef et al. (2006) is common in agricultural systems. This is due to the low variability in the non-irrigated soil where both the N inputs and outputs are reduced. The r^2 meets the criteria only for the irrigated soil.

3.2. Model validation

Figs. 5b, 10, 11, 12 and 13 show ETa, soil moisture and soil N results for the validation period. During this period precipitation was 20% higher compared with 2010/2011, especially during spring in the beginning of the vegetative period (Fig. 1). As a consequence irrigation was 18% lower. N additions with the fertilizer and supplied by the irrigation water were 10% lower than that in the previous period. Also the autumn precipitation events were scarcer leading to the accumulation of NO_3-N in the 60–90 cm, which increased leaching potential. Tables 9 and 10 present the statistics for ETa, soil moisture and soil NO_3-N predictions. As expected, since there was no parameter changing, the statistics show lower values than for calibration. Nevertheless, the trends were predicted ($r^2 \approx 0.8$), the RMSE is often lower than the standard deviation of the measured values and the *D* index is above the minimum required. Again, the worse results were obtained for the nitrate predictions

Table 9
Statistics for the actual evapotranspiration (ETa) prediction for validation (2011/2012).

RMSE (mm)	MSD (mm)	EF	*D*	r^2
0.44	0.74	0.48	0.86	0.77

RMSE per development phase

Development stage	n_{ob}	RMSE (mm)
Initial development	48	0.39
Mid-season	55	0.49
Maturation	28	0.43

RMSE is the root mean squared error, MSD is the mean standard deviation of the measurements, EF is the modeling efficiency, *D* in the *D* index, r^2 is the coefficient of determination, n_{ob} is the number of observations, RMSE is the root mean squared error

Table 10
Statistics for the soil moisture and N predictions for validation (2011/2012).

Depth (cm)	Irrigated area					Non-irrigated area				
	Soil moisture predictions									
	RMSE ($cm^3\ cm^{-3}$)	MSD ($cm^3\ cm^{-3}$)	EF	D	r^2	RMSE ($cm^3\ cm^{-3}$)	MSD ($cm^3\ cm^{-3}$)	EF	D	r^2
0–30	0.029	0.030	0.79	0.83		0.028	0.014	0.73	0.88	
30–60	0.024	0.022	0.77	0.84	0.79	0.021	0.013	0.68	0.69	0.75
60–90	0.020	0.030	0.72	0.88		0.018	0.022	0.30	0.70	
Depth (cm)	Soil N predictions									
	RMSE ($kg\ ha^{-1}$)	MSD ($kg\ ha^{-1}$)	EF	D	r^2	RMSE ($kg\ ha^{-1}$)	MSD ($kg\ ha^{-1}$)	EF	D	r^2
0–60	3.9	13.1	0.91	0.95	0.88	2.2	0.91	−1.89	0.46	0.78
60–90	4.2	7.2	0.83	0.93		3.1	0.92	−1.11	0.70	

RMSE is the root mean squared error, MSD is the mean standard deviation of the measurements, EF is the modeling efficiency, D in the D index, r^2 is the coefficient of determination calculated for the entire profile (0–90 cm).

in the non-irrigated zone probably due to the very low N concentrations in these areas. Overall, the validation results indicate a good model performance for climatic and management conditions different than the ones existing during the calibration period.

3.3. Environmental impacts: soil water and nitrogen balance analysis

3.3.1. Water balance and irrigation

Table 11 shows the predicted water balance for the two experimental years for the irrigated area of one tree, after model calibration and validation. For the two studied periods, ETa accounted for 40 and 42% of the precipitation and irrigation inputs. In 2010/2011, 52% of the inputs were lost by drainage and 8% was stored in the soil profile. In 2011/2012, drainage losses were 62% of the inputs, with depletion of soil water storage. During the olive grove active period, drainage was 71% and 94% of the annual drainage for the 1st and 2nd studied years respectively, being the difference due to distinct precipitation patterns, especially after the irrigation season. During the irrigation periods drainage presented a similar value of 2.9 $m^3\ tree^{-1}$ for both years, corresponding to 57% and 58% of the irrigation inputs. Drainage was essentially due to irrigation since it quantifies as 74% and 61% of the drainage predicted for each active period. The average drainage loss during the irrigation season and for the whole

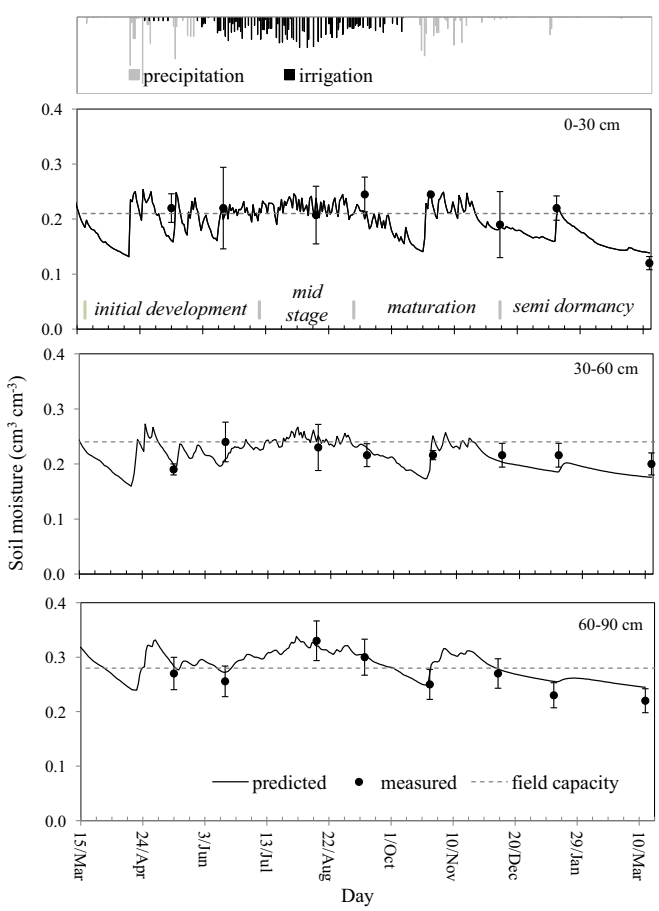

Fig. 10. Predicted and measured soil N-NO_3 in the root zone and in the subjacent layer of the irrigated area for calibration (March 2010–March 2011).

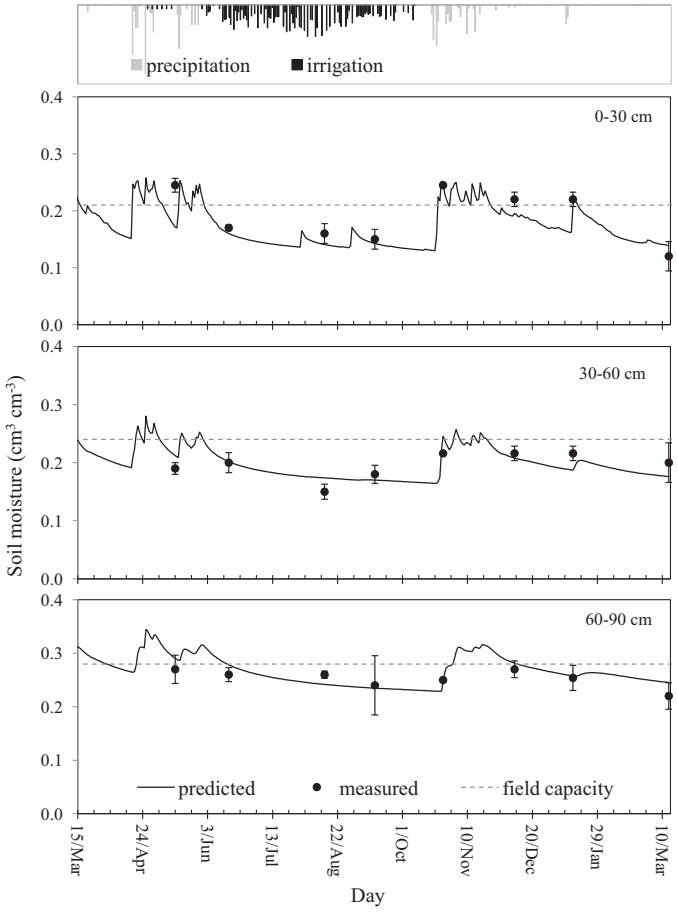

Fig. 11. Predicted and measured soil N-NO_3 in the root zone and in the subjacent layer of the irrigated area for validation (March 2011–March 2012).

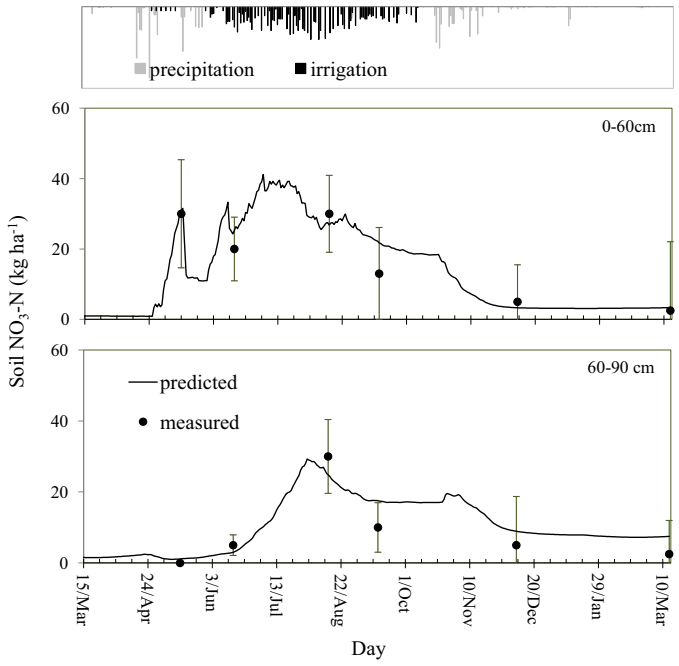

Fig. 12. Predicted and measured soil N-NO_3 in the non-irrigated area for two soil layers for calibration (March 2010–March 2011).

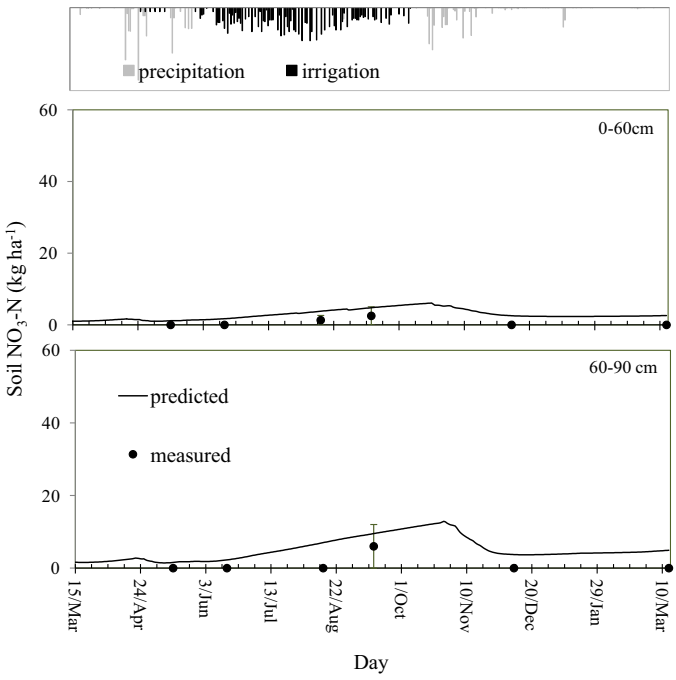

Fig. 13. Predicted and measured soil N-NO_3 in the non-irrigated area for two soil layers for validation (March 2010–March 2011).

field, considering the irrigated and the non-irrigated zones was 135 mm and 96 mm for the 2010/2011 and 2011/2012 periods, respectively. Fig. 14a shows the simulated drainage pattern at the depth of 90 cm under the irrigated and non-irrigated areas for both periods.

3.3.2. *N budget balance and fertilization*

Table 12 presents the predicted nitrogen balance for the 2 years, in grams of mineral N per tree. For both years the non-fertilizer sources of N were higher than the N uptake by the tree, establishing a considerable potential for N loss. The average NO_3-N concentration in the irrigation water (Table 4) yielded an average contribution of 7.7 and 7.1 kg ha^{-1} for each fertigation season, corresponding to 26 and 24 g tree^{-1} respectively. Annual mineralization, equivalent to 33 kg N ha^{-1} year^{-1} and 42 kg N ha^{-1} year^{-1} for the calibration and validation 1 year periods respectively, is within the order of magnitude given by Scheppers and Mosier (1991) (around 20 kg N ha^{-1} year^{-1} per each 1% of soil endogenous OM, for the top 30 cm) and accounted for 47% of the fertilizer inputs. Similar values (44.8–69.6 kg ha^{-1}) were found by Fernández-Escobar et al. (2012) for irrigated olive groves in Mediterranean conditions with similar amounts of OM in the top soil layer. The N loss pathways included leaching and denitrification. The latter represented only 6% of the fertilizer N, which is comparable to other values predicted (Fang et al., 2012) or measured in the field (Meisinger and Randall, 1991), and occurred in the periods during the irrigation season with soil moisture above FC. Table 12 shows that 75% and 64% of the NO_3-N fertilization inputs were leached during the 2010/2011 and 2011/2012 fertigation periods, respectively, which can be related

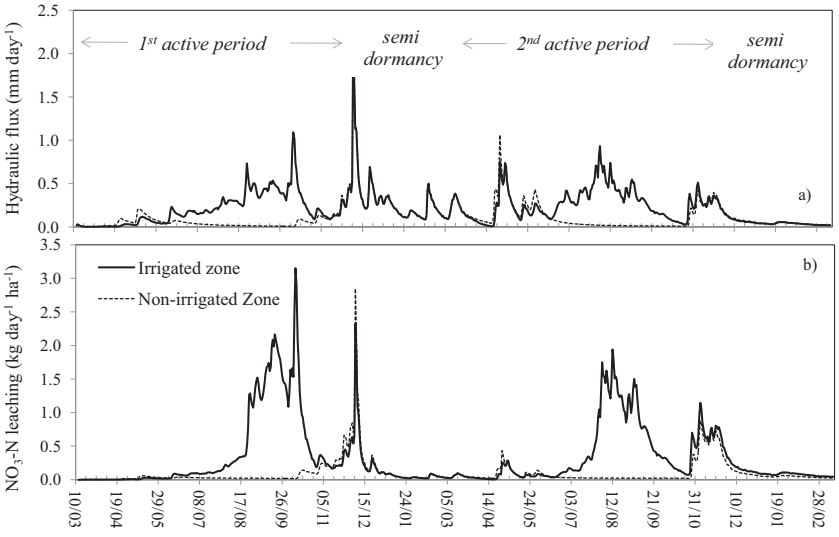

Fig. 14. (a) Hydraulic flux and (b) NO_3-N leaching at the bottom boundary (90 cm), under the irrigated and the non-irrigated areas, for the two studied olive grove cycles.

Table 11
Water balance terms for the soil top 90 cm (all terms in m^3 per tree).

Period	March 2010 to March 2011				
	P	I	ETa	*D*	ΔS
Active	2.48	5.1	3.0	3.9	0.6
Fertigation	0.7	5.1	2.6	2.9	0.2
Dormancy	1.55	0.0	0.12	1.64	−0.12
1-Year tree cycle	4.04	5.1	3.12	5.53	0.5
Period	March 2011 to March 2012				
	P	I	ETa	*D*	ΔS
Active	2.6	4.8	3.1	4.6	−0.2
Fertigation	0.1	4.8	2.1	2.8	−0.1
Dormancy	0.2	0.0	0.1	0.3	−0.2
1-Year tree cycle	2.8	4.8	3.2	4.9	−0.4

P is the precipitation, I is the irrigation, ETa is the actual evapotranspiration, *D* is the deep drainage, ΔS is the storage variation for the period.

Table 12
Mineral N budget for the top 90 cm (all terms in g $tree^{-1}$).

Period	March 2010 to March 2011							
	N_{min}	N_F	N_I	N_{upt}	N_{leach}	N_{den}	N_{res}	ΔS
Active	102	217	26	100	218	12	17	15
Fertigation	72	217	26	88	162	8	72	55
1-Year tree cycle	124	217	26	100	233	12	9	8
Period	March 2011 to March 2012							
	N_{min}	N_F	N_I	N_{upt}	N_{leach}	N_{den}	N_{res}	ΔS
Active	117	228	24	102	204	7	42	33
Fertigation	85	228	24	97	145	4	122	86
1-Year tree cycle	140	228	24	102	230	10	37	28

ΔS is the variation in mineral N storage, N_F is N added with the fertilization, N_I is the nitrogen source in the irrigation water, N_{min} is the mineralization of organic N, N_{upt} is the N uptake by the olive trees, N_{leach} is the N lost by leaching, N_{den} are the N losses by denitrification and N_{res} is the residual NO_3-N.

to the occurrence of drainage fluxes from the irrigation events as well as to the NO_3-N storage surplus in the soil. As a result, at the end of the fertigation season the residual N in the profile was reasonably low (corresponding to 21 and 36 kg NO_3-N ha^{-1}). Only 45% of the fertilizer inputs were used by the trees during the fertigation period. The leaching losses for the total area, averaged from the irrigated and the non-irrigated areas, were 51 kg NO_3-N ha^{-1} and 49 kgNO_3-N ha^{-1} for the 2010/2011 and 2011/2012 periods, respectively. Fig. 14b shows the daily leaching rate at the depth of 0.9 m under the irrigated and non-irrigated areas for both periods, closely following the drainage pattern (Fig. 14a). Average NO_3-N concentrations in the drainage water were estimated by taking into account the drainage volume out of the root zone and the amount of N leached and presented values of 55.8 and 44.3 mg NO_3-N L^{-1} for each studied year. Fernández-Escobar et al. (2012) estimated average NO_3-N concentrations in the drainage water between 50 and 150 mg NO_3-N L^{-1} for an application rate of 1.15 kg N $tree^{-1}$. Although these concentrations will be diluted in the groundwater, the accumulated impact of this surplus in the context of long-term productivity leads to a potential groundwater contamination risk. The results of this study demonstrate that opportunities exist to improve the performance of the drip fertigation system.

3.3.3. *Optimization of irrigation and N fertilization practices for the reduction of environmental impacts*

The calibrated and validated RZWQM2 was used to test the effects of different irrigation management scenarios on drainage losses and N leaching. Three scenarios were analyzed, corresponding to a full irrigation (FIFC) scheme based upon the model estimation of ETp and two regulated deficit irrigation (RDI) scheme, according to the work of Gispert et al. (2011). The scenarios were: (i) FIFC – full irrigation, where the atmospheric demand of the trees was met and the application frequency maintained the water storage below the soil field capacity (FC); (ii) RDI75 – regulated deficit irrigation, where the irrigation amount between mid-July (stone hardening) and mid-September (onset of ripening) was 75% of FI for the same period. For the rest of the season (March to July and late September and October), RDI received the same amounts of water than FI; (iii) RDI50 – similar to RDI75, but the reduction during the deficit period is 50% in relation to the FI.

Results are shown in Table 13 and refer to the fertigation period (April to October). Compared with the experiment, the FIFC scenario resulted in irrigation water saving of 51% without any reduction in ETa, whereas drainage was reduced by 47%. Drainage due to irrigation was now only 13% of total drainage compared with 56% for the experiment. N leaching was reduced by 90% and consequently N uptake increased by 31%. The higher soil aeration in relation to the experiment resulted in 75% decrease in denitrification and 13% increase in mineralization. However, the residual N content of the profile at the end of the fertigation season increased. When compared with FIFC, the RDI75 and RDI50 scenarios presented 13% and 27% water savings respectively, whereas the ETa decreased 5% and 10%, which in this period has minimum impacts upon production and oil quality. Drainage during the irrigation season was reduced by 15% and 28%, respectively. As a consequence N leaching decreased 31 and 68%, respectively, and N accumulated in the profile. In the absence of drainage fluxes this N can be used later, otherwise it will be leached. N additions through mineralization increased 19% for the RDI75 and decreased 11% for the RDI50. This is according to the fact that mineralization is optimized for soil moisture between FC and 40% FC (Campbell and Biederbeck, 1982). In relation to FIFC, N uptake decreased by 19% in both deficit irrigation scenarios. For the RDI scenarios the main contribution to reducing NO_3-N leaching loss was the reduction of drainage flow. However, due to the existence of an N surplus, the residual profile of N at the end of this period was high representing an important leaching potential. Fernández-Escobar et al. (2009) measured similar residual soil N profiles for 0 and 1.15 kg N $tree^{-1}$ $year^{-1}$ application rates. A simple balance between the uptake needs and the inputs show that the non-fertilizer sources of N (OM mineralization and the irrigation water contribution) are sufficient. With the objective of satisfying N uptake needs but minimizing the leaching and residual soil N (at end of the fertigation season left-over soil N), three levels of fertilization were studied for each irrigation scenarios, 100%, 50% and 0% of the original application to compare NO_3-N loss at the same drainage flow. Table 13 shows that, for each irrigation scenario, soil residual N can be minimized at the expense of an N uptake decrease between 3 and 13% for the 50% application and between 20 and 30% for the 0% application. This shows that once the drainage fluxes are controlled by an optimized irrigation scheme, soil N surplus has to be minimized by applying the fertilizer exactly when needed, using a real time plant N indicator, *e.g.* previous season's foliar analysis or a chlorophyll meter.

Further research will allow the scaling-up of the NO_3^- leaching from different irrigated olive orchards to all of the area occupied by the intensive and super intensive olive groves in Alentejo region. This study could be based on an approach combining the groundwater recharge quantification for site specific hydrogeological properties, and satellite-based surface energy balance models to map actual crop ET.

Table 13
Results for the management scenarios (fertigation season).

Irrigation	N_F	I (m^3 $tree^{-1}$)	ETa (m^3 $tree^{-1}$)	D (m^3 $tree^{-1}$)	N_I (g $tree^{-1}$)	N_{min} (g $tree^{-1}$)	N_{upt} (g $tree^{-1}$)	N_{leach} (kg ha^{-1})	N_{den} (kg ha^{-1})	N_{res} (kg ha^{-1})
FIFC	100%	2.59	2.98	1.53	12.6	81	115	16	2	62
	50%					81	94	14	1	48
	0%					83	80	14	1	11
RDI75	100%	2.25	2.83	1.30	11.3	96	93	11	2	69
	50%					85	86	11	1	36
	0%					95	75	11	1	11
RDI50	100%	1.90	2.71	1.10	9.5	72	94	5	2	70
	50%					77	91	5	1	39
	0%					73	71	5	1	11

I is the irrigation, ETa is the actual evapotranspiration, D is the deep drainage; N_F is N added with the fertilization, N_I is the nitrogen source in the irrigation water, N_{min} is the mineralization of organic N, N_{upt} is the N uptake by the olive trees, N_{den} are the N losses by denitrification and N_{leach} is the N lost by leaching, N_{res} is the N residual profile.

4. Conclusions

RZWQM2 was adapted for the representation of olive groves under a typical Mediterranean agro-ecosystem, resulting in a more appropriate description of LAI with positive impacts upon the canopy boundary layer resistance and the bulk stomatal resistance of the canopy for the ETp calculation.

The model was able to predict the water and N dynamics in the fertigated olive orchards yielding the expected statistics to meet the acceptance criteria with respect to ETa, soil moisture and soil NO_3-N for the calibration and validation phases. Modeling uncertainty could further be reduced if root N uptake data were available to validate the predictions. The model was considered acceptable for predicting drainage and N leaching, however it is advisable to calibrate the estimated hydraulic properties against a simple infiltration redistribution experiment.

The analyses of the current practices showed irrigation to be excessive since soil moisture equaled or exceeded FC during an important part of the irrigation season causing downward fluxes out of the root zone. Model predictions showed that 57% and 58% of the irrigation inputs were lost by drainage during the irrigation season, for the 2010/2011 and 2011/2012 olive grove cycles, respectively. Leaching of N was 75% and 66% of the fertilization inputs for the same periods. A simple N balance showed that the inputs exceeded crop N uptake producing a N surplus with a high leaching potential. The accumulated impact of the surplus can be considerable in the context of long-term productivity, environment and human health, consisting in a potential groundwater contamination risk.

Our results, together with other recent findings on the effect of water stress on olive fruit development show that both the RDI75 and RDI50 treatments seem appropriate for a sustainable fertigation management in the studied olive orchards. These RDI strategies would require total amounts of 670 and 565 m^3 ha^{-1} respectively compared with the 1500 m^3 ha^{-1} currently applied. However, both the amount and frequency of irrigation will depend upon the precipitation occurring during the deficit period, requiring a real time field management. As to the N management, RDI75 creates soil moisture conditions that optimize mineralization, reducing the fertilizer needs. The considerable amount of non-fertilizer N sources indicates that a small amount of fertilizer will be needed and the application time should be decided based upon crop N demand in order to minimize soil residual N in the profile.

Acknowledgements

This study was supported by the project PTDC/AAC – AMB/100635/2008 funded by "Fundação para a Ciência e a Tecnologia", Portugal. Thanks are due to Mr. Nuno Conceição for the help with the irrigation data collection and Ms Emilia Silva and Dr Michiel Dam for the help with the soil sampling.

References

Ahuja, L.R., Johnsen, K.E., Rojas, K.W., 2000a. Water and chemical transport in soil matrix and macropores. In: Ahuja, L.R., et al. (Eds.), The Root Zone Water Quality Model. Water Resources Publ., Highlands Ranch, CO, pp. 13–50.
Ahuja, L.R., Naney, J.W., Williams, R.D., 1985. Estimating soil water characteristics from simpler properties or limited data. Soil Sci. Am. J. 49, 1100–1105.
Ahuja, L.R., Rojas, K.W., Hanson, J.D., Shaffer, M.J., Ma, L. (Eds.), 2000b. The Root Zone Water Quality Model. Water Resources Publ., Highlands Ranch, CO.
Allen, R., Pereira, L.S., Raes, D., Smith, M., 1998. Crop Evapotranspiration. Guidelines for Computing Crop Water Requirements. FAO, Rome, FAO Irrigation and Drainage Paper 56.
Azevedo, A.L., Cary, L.C., 1989. Problemas e potencialidades da agricultura portuguesa, com ênfase especial para o Alentejo, n "Cooperação luso-alemã entre Universidades no domínio da investigação agrária aplicada – Resultados de projectos de investigação agrária". Vila Real, 135–161.
Bonachela, S., Orgaz, F., Villalobos, F.J., Fereres, E., 2001. Soil evaporation from drip-irrigated olive orchards. Irrig. Sci. 20 (2), 65–71.
Bouwer, H., 1986. Intake rate: cylinder infiltrometer. In: Klute, A. (Ed.), Methods of Soil Analysis. Part 1. , 2nd ed. ASA and SSSA, Madison, WI, pp. 825–844, Agron. Monogr. 9.
Brisson, N., Mary, B., Ripoche, D., Jeuffroy, M.H., Ruget, F., Nicoullaud, B., Delécolle, R., 1998. STICS: a generic model for the simulation of crops and their water and nitrogen balances. I. Theory and parameterization applied to wheat and corn. Agronomie 18 (5–6), 311–346.
Cameira, M.R., Ahuja, L., Fernando, R.M., Pereira, L.S., 2000. Evaluating field measured soil hydraulic properties in water transport simulations using the RZWQM. J. Hydrol. 236 (1–2), 78–90.
Cameira, M.R., Fernando, R.M., Ahuja, L.R., Ma, L., 2007. Using RZWQM to simulate the fate of nitrogen in field soil–crop environment in the Mediterranean region. Agric. Water Manage. 90 (1), 121–136.
Cameira, M.R., Fernando, R.M., Ahuja, L., Pereira, L., 2005. Simulating the fate of water in field soil–crop environment. J. Hydrol. 315 (1), 1–24.
Cameira, M.R., Tedesco, S., Leitão, T.E., 2014. Water and nitrogen budgets under different production systems in Lisbon urban farming. Biosyst. Eng. 125, 65–70.
Campbell, C.A., Biederbeck, V.O., 1982. Changes in mineral N and numbers of bacteria and actinomycetes during two years under wheat-fallow in Southwestern Saskatchewan. Can. J. Soil Sci. 62, 125–137.
Campbell, G.S., 1974. A simple method for determining unsaturated conductivity from moisture retention data. Soil Sci. 117, 311–314.
Celia, M.A., Bouloutas, E.T., Zarba, R.L., 1990. A general mass-conservative numerical solution for the unsaturated flow equation. Water Resour. Res. 26, 1483–1496.
Conceição, N., Ferreira, M.I., 2013. Caracterização do uso da água pelos olivais. In: PTDC/AAC – AMB/100635/2008. WUSSIAME-Uso da água, estratégias de sobrevivência hídrica e impacto de agroquímicos nos recursos hídricos em ecossistemas agrícolas mediterrânicos, Project Final Report (in Portuguese).
Er-Raki, Chehbounib, S., Bouletb, A., Williamsc, D.G., 2010. Using the dual approach of FAO-56 for partitioning ET into soil and plant components for olive orchards in a semi-arid region. Agric. Water Manage. 97, 1769–1778.
Fang, Q.X., Malone, R.W., Ma, L., Jaynes, D.B., Thorp, K.R., Green, T.R., Ahuja, L.R., 2012. Modeling the effects of controlled drainage, N rate and weather on nitrate loss to subsurface drainage. Agric. Water Manage. 103, 150–161.
FAO, 2006. World Reference Base for Soil Resources. World Soil Resources Reports. Food and Agriculture Organization of the United Nations, Rome.
FAOSTAT, 2012. http://faostat.fao.org
Farahani, H.J., DeCoursey, D.G., 2000. Evaporation and transpiration processes in the soil-residue-canopy system. In: Ahuja, L.R., et, al. (Eds.), The Root Zone Water Quality Model. Water Resources Publ., Highlands Ranch, CO, pp. 51–80.
Fernández, J.E., Moreno, F., Cabrera, F., Arrue, J.L., Martín-Aranda, J., 1991. Drip irrigation, soil characteristics and the root distribution and root activity of olive trees. Plant Soil 133 (2), 239–251.
Fernández-Escobar, R., García-Novelo, J.M., Molina-Soria, C., Parra, M.A., 2012. An approach to nitrogen balance in olive orchards. Sci. Hortic. 135, 219–226.
Fernández-Escobar, R., Marin, L., Sánchez-Zamora, M.A., García-Novelo, J.M., Molina-Soria, C., Parra, M.A., 2009. Long-term effects of N fertilization on cropping and

growth of olive trees and N accumulation in soil profile. Eur. J. Agron. 31 (4), 223–232.
Ferreira, M.I., Paço, T.A., Silvestre, J., 2004. Combining techniques to study evapotranspiration in woody crops: application to small areas – two case studies. Acta Hortic. (ISHS) 664, 225L 232.
Follet, R., Shaffer, M., Brodhal, M., Reichman, G., 1994. NLEAP simulation of residual soil nitrate for irrigated and non-irrigated corn. J. Soil Water Conserv. 49 (4), 375–382.
Gärdenäs, A.I., Hopmans, J.W., Hanson, B.R., Šimůnek, J., 2005. Two-dimensional modeling of nitrate leaching for various fertigation scenarios under micro-irrigation. Agric. Water Manage. 74 (3), 219–242.
Gispert, J.R., de Cartagena, F.R., Villar, J.M., Girona, J., 2013. Wet soil volume and strategy effects on drip-irrigated olive trees (cv. 'Arbequina'). Irrig. Sci., 1–11.
Goldhamer, D.A., 1999. Regulated deficit irrigation for California canning olives. Acta Hortic. 474, 369–372.
Green, W.H., Ampt, G.A., 1911. Studies on soil physics. 1. Flow of air and water through soils. J. Agric. Sci. 4, 1–24.
Hansen, S., Jensen, H.E., Nielsen, N.E., Svendsen, H., 1990. DAISY: a soil plant system model. Danish simulation model for transformation and transport of energy and matter in the soil plant atmosphere system. Fertil. Res. 27, 141–149.
Hansen, T.L., Bhander, G.S., Christensen, T.H., Bruun, S., Jensen, L.S., 2006. Life cycle modelling of environmental impacts of application of processed organic municipal solid waste on agricultural land (EASEWASTE). Waste Manage. Res. 24 (2), 153–166.
Heinen, M., 2001. FUSSIM2: brief description of the simulation model and application to fertigation scenarios. Agronomie 21 (4), 285–296.
Hutson, J.L., Wagenet, R.J., 1995. A multi region model describing water flow and solute transport in heterogeneous soils. Soil Sci. Am. J. 59 (3), 743–751.
Iniesta, F., Testi, L., Orgaz, F., Villalobos, F.J., 2009. The effects of regulated and continuous deficit irrigation on the water use, growth and yield of olive trees. Eur. J. Agron. 30 (4), 258–265.
Jansson, P.E., Karlberg, L., 2004. Coupled heat and mass transfer model for soil–plant–atmosphere systems. Royal Institute of Technology, Department of Civil and Environmental Engineering, Stockholm, pp. 435.
Lavee, S., Wodner, M., 1991. Factors affecting the nature of oil accumulation in fruit of olive (*Olea europaea* L.) cultivars. J. Hortic. Sci., 66.
Ma, L., Ahuja, L.R., Nolan, B.T., Malone, R.W., Trout, T.J., Qi, Z., 2012. Root Zone Water Quality Model (RZWQM2): model use, calibration and validation. Trans. ASABE 55, 1425–1446.
Ma, L., Ahuja, L.R., Saseendran, S.A., Malone, R.W., Green, T.R., Nolan, B.T., Bartling, P.N.S., Flerchinger, G.N., Boote, K.J., Hoogenboom, G., 2011. A Protocol for parameterization and calibration of RZWQM2 in field research. In: Ahuja, L.R., Ma, L. (Eds.), Methods 754 of Introducing System Models into Agricultural Research. SSSA Book Series, pp. 1–64, Madsion, WI.
Ma, L., Ahuja, L.R., Malone, R.W., 2007. Systems modeling for soil and water research and management: current status and needs in the 21st century. Trans. ASABE 50, 1705–1713.
Mariscal, M.J., Orgaza, F., Villalobos, F.J., 2000. Modelling and measurement of radiation interception by olive canopies. Agric. For. Meteorol. 100, 183–197.
Massoud, M.A., Scrimshaw, M.D., Lester, J.N., 2003. Qualitative assessment of the effectiveness of the Mediterranean action plan: wastewater management in the Mediterranean region. Ocean Coast. Manage. 46, 875–899.
Maynard, D., Kalra, Y., 1993. Nitrate and exchangeable ammonium nitrogen. In: Carter, M. (Ed.), Soil Sampling and Methods of Analysis. Canadian Society of Soil Science, pp. 25–38.
Meisinger, J.J., Randall, G.W., 1991. Estimating nitrogen budgets for soil–crop systems. In: Follett, R.F., Kenney, D.R., Cruse, R.M. (Eds.), Managing Nitrogen for Ground-Water Quality and Farm Profitability. Soil Science Society of America, Madison, pp. 85–122.
Morales-Sillero, A., Fernández, J.E., Ordovás, J., Suárez, M.P., Pérez, J.A., Liñán, J., Troncoso, A., 2009. Plant–soil interactions in a fertigated 'Manzanilla de Sevilla' oliveorchard. Plant Soil 319 (1–2), 147–162.
Nash, J.E., Sutcliffe, J.V., 1970. River flow forecasting through conceptual models. Part 1. A discussion of principles. J. Hydrol. 10, 282–290.
Nimah, M., Hanks, R., 1973. Model for estimating soil-water-plant-atmospheric interrelation. I. Description and sensitivity. Soil Sci. Soc. Am. Proc. 37,9 522–527.
Nolan, Puckett, B.T., Ma, L.J., Green, L., Bayless, C.T., MaloneR.W., E.R., 2010. Predicting unsaturated zone nitrogen mass balances in diverse agricultural settings of the United States. J. Environ. Qual. 39, 1051–1065.
Orgaz, F., Fereres, E., 2004. Riego. In: Barranco, D., Fernández-Escobar, R., Rallo, L. (Eds.), El cultivodelolivo. Mundi Prensa, Madrid, pp. 323–346.
Paço, T.A., Ferreira, M.I., Rosa, R., Paredes, P., Rodrigues, G., Conceição, N., Pacheco, C., Pereira, L.S., 2012. The dual crop coefficient approach using a density factor to simulate the evapotranspiration of a peach orchard: SIMDualKc model vs. eddy covariance measurements. Irrig. Sci. 30, 115L 126.
Ramos, F., Santos, F.L., 2010. Yield and olive oil characteristics of a low-density orchard (cv. Cordovil) subjected to different irrigation regimes. Agric. Water Manage. 97, 363–373.
Rawls, W.J., Brakensiek, D.L., Saxton, K.E., 1982. Estimation of soil water properties. Trans. ASAE 25, 1316–1320.
RGA2009, 2011. Agricultural Census 2009. Instituto nacional de estatística, Lisbon, Portugal.
Scheppers, J., Mosier, A., 1991. Accounting for N in nonequilibrium soil–crop systems. In: Follet, R.F., Keeney, D.R., Cruse, R.M. (Eds.), Managing N for Ground Water Quality and Farm Profitability. Soil Science Society of America, Madison, WI, pp. 125–138.
Shaffer, M.J., Rojas, K.W., DeCoursey, D.G., Hebsen, C.S., 2000. Nutrient chemistry processes – OMNI. In: Ahuja, L.R., et, al. (Eds.), The Root Zone Water Quality Model. Water Resources Publ., Highlands Ranch, CO, pp. 119–144.
Shuttleworth, W.J., Wallace, J.S., 1985. Evaporation from sparse crops – an energy combination approach. Q. J. R. Met. Soc. 111, 839–855.
Silva, R.M., Paço, T.A., Ferreira, M.I., Oliveira, M., 2008. Transpiration of a kiwifruit orchard estimated using the Granier sap flow method calibrated under field conditions. Acta Hortic. (ISHS) 792, 593–600.
Šimůnek, J., Šejna, M., van Genuchten, M.Th., 1999. The HYDRUS-2D Software Package for Simulating Two-Dimensional Movement of Water, Heat, and Multiple Solutes in Variably Saturated Media. Version 2.0, IGWMC-TPS-53. International Ground Water Modeling Center, Colorado School of Mines, Golden, CO, pp. 251.
Testi, L., Villalobos, F.J., Orgaz, 2004. Evapotranspiration of a young irrigated olive orchard in southern Spain. Agric. For. Meteorol. 121, 1–18.
Tognetti, R., d'Andria, R., Lavini, A., Morelli, G., 2006. The effect of deficit irrigation on crop yield and vegetative development of *Olea europaea* L. (cvs. Frantoio and Leccino). Eur. J. Agron. 25, 356–364.
Torres-Ruiz, J.M., Diaz-Espejo, A., Morales-Sillero, A., Martín-Palomo, M.J., Mayr, S., Beikircher, B., Fernández, J.E., 2013. Shoot hydraulic characteristics, plant water status and stomatal response in olive trees under different soil water conditions. Plant Soil, 1–11.
Tovar, M.J., Romero, P.M., Alegre, A., Girona, J., Motilva, M.J., 2002. Composition and organoleptic characteristics of oil from Arbequina olive trees under deficit irrigation. J. Sci. Food Agric. 82, 1755–1763.
Villalobos, F.J., Orgaz, F., Testi, L., Fereres, E., 2000. Measurement and modeling of evapotranspiration of olive (*Olea europaea* L.) orchards. Eur. J. Agron. 13 (2), 155–163.
Warrick, A.W., Mullen, G.J., Nielsen, D.R., 1977. Scaling field measured soil hydraulic properties using a similar media concept. Water Resour. Res. 13, 355–362.
Willmott, C.J., 1981. On the validation of models. Phys. Geogr. 2, 184–194.
Xiloyannis, C., Celano, G., Palese, A.M., Dichio, B., Nuzzo, V., 2000. Mineral nutrients uptake from the soil in irrigated olive trees, cultivar coratina, over six years after planting. Acta Hortic. 586, 453–456.
Youssef, M.A., Skaggs, R.W., Chescheir, G.M., Gilliam, J.W., 2006. Field evaluation of a model for predicting nitrogen losses from drained lands. J. Environ. Qual. 35 (6), 2026–2042.